Simplified Lateral Torsional Buckling Equations for Singly-Symmetric I-Section Members

by

Donald W. White
Professor
Structural Engineering, Mechanics and Materials

and

Se-Kwon Jung
Graduate Research Assistant

Structural Engineering, Mechanics and Materials
Report No. 03-24b

School of Civil and Environmental Engineering
Georgia Institute of Technology
Atlanta, GA 30332-0355
e-mail: dwhite@ce.gatech.edu
Phone: 404-894-5839
FAX: 404-894-0278

March 2003

Simplified Lateral Torsional Buckling Equations for Singly-Symmetric I-Section Members

DONALD W. WHITE and SE KWON JUNG

Donald W. White is Professor, Structural Engineering, Mechanics and Materials,
Georgia Institute of Technology, Atlanta, GA 30332-0355

Se Kwon Jung is Graduate Research Assistant, Structural Engineering, Mechanics and Materials,
Georgia Institute of Technology, Atlanta, GA 30332-0355

INTRODUCTION

In the companion paper (White and Jung 2003a), the authors develop and discuss the advantages of a recommended set of equations for the elastic lateral-torsional buckling (LTB) resistance of I- and channel-section members. These equations are utilized as the base elastic LTB expressions within the AASHTO (2004) and AISC (2005) Specifications. White and Jung (2003a) focus on the characteristics of the recommended equations pertaining to doubly-symmetric I-section members and channels. This paper extends these developments to singly-symmetric I-section members, including composite I-sections in negative bending and channel-capped I-sections. Two approaches are highlighted for calculation of the elastic LTB resistance of these general member types:

1. Ad hoc application of the doubly-symmetric equations recommended in (White and Jung 2003a), similar to the approach taken in AASHTO (1998) using an alternative set of LTB equations for doubly-symmetric I-section members.
2. A simplified form of the rigorous equations obtained from open-walled section beam theory.

A key advantage of the first approach is that it leads to a single set of equations for all I-section members and channels. Also, these equations are simpler to apply than the rigorous beam theory equations for general I-shapes. As noted in (White and Jung 2003a) and demonstrated in this paper, the recommended doubly-symmetric equations give an improved approximation of the rigorous beam theory solution for singly-symmetric I-section members compared to the AASHTO (1998) equations. Also, as explained in this paper, these equations can be applied as a conservative but typically adequate approximation of the elastic LTB resistance for composite I-section members in negative bending. The main disadvantage of the first approach is that it is not rigorous. In as such, the behavior of the equations must be studied parametrically to ensure that they predict the physical strengths adequately for all practical singly-symmetric geometries. Any ranges of parameters that produce unacceptable error must be disallowed.

The key advantage of the second approach is that an exact or a highly accurate approximation of the beam theory LTB resistance is obtained. The primary disadvantage of this approach is that the equations are more complex. Also, their extension to the handling of composite I-girders in negative bending is not as straightforward.

CONTEXT

The LTB provisions in AASHTO (1998 and 2004) and AISC (1999 and 2005) are based on the logic of identifying the two anchor points shown in Fig. 1 for the base case of uniform major-axis bending. Anchor point 1 is located at the length $L_b = L_p$ corresponding to development of the maximum potential flexural resistance under uniform major-axis bending (labeled as the compression flange stress F_{max} or the bending moment M_{max} in the figure). Anchor point 2 is located at the smallest length $L_b = L_r$ for which the LTB strength is governed by elastic buckling. The corresponding base moment and compression flange elastic stress levels are denoted in this paper by the symbols M_{yr} and F_{yr}, where $M_{yr} = F_{yr} S_{xc}$ and F_{yr} is the compression flange flexural stress corresponding to the nominal onset of yielding within the cross-section (in tension or compression), including compression flange residual stress effects. The equivalent terms in AISC (1999) are represented by the symbols F_L and M_r. The parameter L_r is obtained generally as the length associated with elastic buckling at a compression flange major-axis bending stress of $F_{cr} = F_{yr}$. The anchor points in Fig. 1 subdivide the LTB problem into three regions, the "compact" or "plastic buckling" region, the "noncompact" or "inelastic buckling" region, and the "slender" or "elastic buckling" region. This is a powerful approach for quantifying the general LTB resistance in that it facilitates the handling of a number of complex issues for general cross-sections. This approach is the framework for the discussion of the elastic LTB equations in this paper.

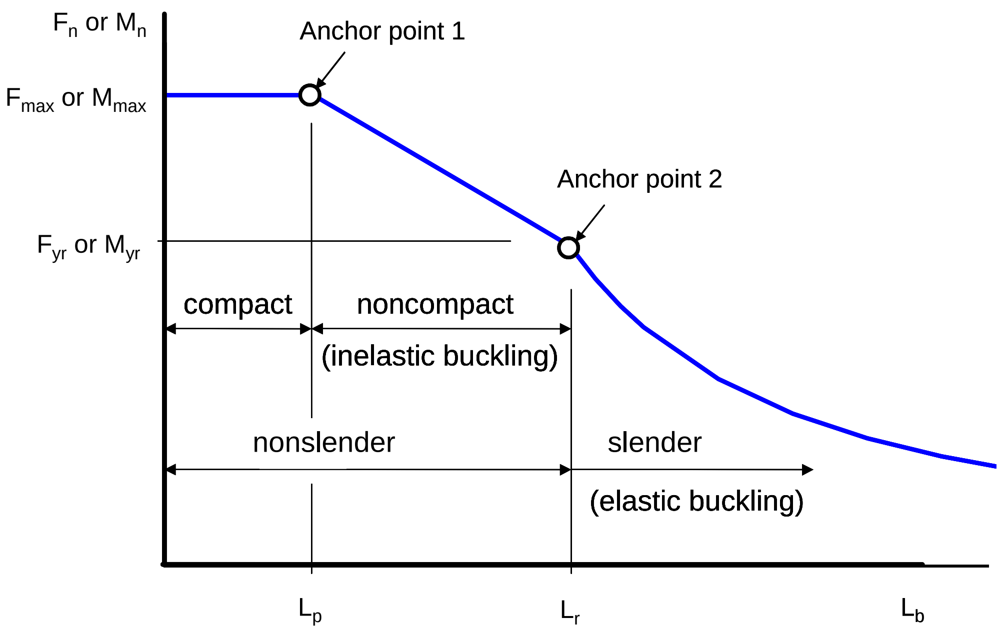

Figure 1. Basic form of the LTB provisions in AASHTO (1998 and 2004) and AISC (1999 and 2005) corresponding to uniform major-axis bending ($C_b = 1$).

ORGANIZATION

This paper first summarizes the basic doubly-symmetric LTB equations from AASHTO (1998) and from (White and Jung 2003a) as well as the exact beam theory equations for a general singly-symmetric noncomposite member. Next, a simplified form of the rigorous solution for the LTB resistance of a noncomposite singly-symmetric I-section member is suggested, and a minor change is proposed to an approximate equation for a key coefficient pertaining to the cross-section monosymmetry for rectangular-flange members. In AISC (1999), no explicit L_r equation is provided for singly-symmetric I-section members. As a result, engineers have often assumed that L_r must be calculated iteratively. To address this problem, an explicit expression for L_r is derived based on the above rigorous LTB solution.

The paper then compares the suggested rigorous beam theory expression for the LTB resistance to the equation employed in AISC (1999), and also to a special form of the LTB equations in which the strength is written in the form of Euler's equation for the column buckling stress using an equivalent radius of gyration r_E. Although this later form does not result in any significant simplification of the LTB calculations, it facilitates the understanding of the radius of gyration parameter r_t employed within the suggested doubly-symmetric LTB equations. The paper devotes one section to an explanation of the relationships between r_E and r_t for a general singly-symmetric I-section. Lastly, the rigorous beam theory equations are considered in the limit that J (or JL_b^2) is taken equal to zero. As explained in the companion paper, this assumption is invoked commonly for slender-web I-section members and in considering the idealized behavior at $L_b = L_p$.

Given the above equations, a primary contribution of the paper is the evaluation of the accuracy of: (1) the doubly-symmetric equations from AASHTO (1998), (2) the doubly-symmetric equations recommended by White and Jung (2003a) and (3) the rigorous form of the singly-symmetric equations suggested in this paper, for a comprehensive practical range of singly-symmetric rectangular-flange I-sections. Comparisons are made to the exact solutions from open-walled section beam theory.

The paper concludes with a summary assessment of the two recommended approaches for quantifying the elastic LTB resistance of general I-section members. The rationale for the ad hoc application of the doubly-symmetric equations to composite I-girders in negative bending and to channel-capped I-sections is explained and several specific examples are presented. Limits are suggested for the applicability of the recommended equations.

The influence of web distortion on the LTB strength, and the corresponding implications relative to the use of beam-theory based formulae, are addressed by White and Jung (2003b).

AASHTO (1998) AND RECOMMENDED EQUATIONS FOR F_{cr} – DOUBLY-SYMMETRIC I-SECTION MEMBERS

The AASHTO LRFD (1998) Specifications utilize the following formula to quantify the elastic LTB strength of noncomposite I-beams and girders with compact and noncompact webs, and as well as the strength of noncomposite girders with longitudinally-stiffened webs:

$$M_{cr} = C_b \frac{3.14E}{L_b} I_{yc} \sqrt{9.87\left(\frac{h}{L_b}\right)^2 + 0.769\frac{J}{I_{yc}}} \tag{1}$$

This equation is exact only for doubly-symmetric I-section members; however, it is also utilized in the AASHTO Specifications for singly-symmetric sections. The commentary of these Specifications states that Eq. (1) gives predictions within approximately 10 percent of the results from the singly-symmetric I-section LTB equations in AISC (1999).

Although Eq. (1) performs reasonably well for a large number of practical singly-symmetric I-shapes, it exhibits significant errors relative to the rigorous beam theory strengths in certain cases. This is in part due to the fact that if the above equation is used, changes in the size of the tension flange and web influence the LTB strength only through the terms h and J. An alternative simple equation that exhibits better accuracy than Eq. (1), and which has a number of other advantages relative to the AASHTO (1998) equation, is (White and Jung 2003a)

$$F_{cr} = C_b \frac{\pi^2 E}{(L_b / r_t)^2} \sqrt{1 + 0.078 \frac{J}{S_{xc} h} (L_b / r_t)^2} \tag{2}$$

where

$$r_t \cong \frac{b_{fc}}{\sqrt{12\left(\frac{h}{d} + \frac{1}{3}\frac{A_{wc}}{A_{fc}}\frac{D^2}{hd}\left(1 + 6\frac{A_{fillet}}{A_{wc}}\right)\right)}} \tag{3}$$

This is a useful form of the fundamental elastic LTB resistance for a doubly-symmetric I-shape, expressed in terms of the flange vertical bending stress. All of the variables in this equation are well known in terms of their physical significance, and are readily available or easily calculated during the design process. If the approximation $d \cong h \cong D$ is invoked, Eq. (3) reduces to the radius of gyration of the compression flange plus one-third of the area of the web in compression. However, White and Jung (2003a) recommend the direct use of Eq. (3) with Eq. (2), since Eq. (2) is exact for all practical purposes in this case whereas the above approximation is more than 10 percent conservative for some of the heaviest column-type W sections. Equation (2) shows that the fundamental elastic LTB strength is simply a function of the elastic modulus E, the slenderness L_b/r_t, the ratio of the torsional and major-axis bending efficiencies $\frac{J}{S_{xc}h}$, and the moment gradient modifier C_b. Also, when the second term under the radical is small relative to one, Eq. (2) reduces to the form

$$F_{cr} = C_b \frac{\pi^2 E}{(L_b / r_t)^2} \tag{4}$$

If Eq. (2) is used for the elastic LTB strength, this expression can be equated to F_{yr} for the case of uniform major-axis bending ($C_b = 1$) and solved for the root of the resulting quadratic equation for L_r^2 (i.e., a quartic equation for L_r) to obtain

$$L_r = 1.95 r_t \frac{E}{F_{yr}} \sqrt{\frac{J}{S_{xc} h}} \sqrt{1 + \sqrt{1 + 6.76\left(\frac{F_{yr}}{E}\frac{S_{xc} h}{J}\right)^2}} \tag{5}$$

whereas for slender-web I-sections, in which J is taken as zero, the result based on Eq. (4) is simply

$$L_{r(J=0)} = \pi r_t \sqrt{\frac{E}{F_{yr}}} \tag{6}$$

It should be noted that although Eq. (5) is a relatively long equation involving embedded square root operations, the variables in this equation are few in number ($\frac{E}{F_{yr}}$, $\frac{S_{xc}h}{J}$ and r_t) and are easily calculated or are readily available within the design process. Also, L_r is directly proportional to r_t. White and Jung (2003a) show that r_t is the radius of gyration that is most fundamental to the LTB of I-section members. The variable r_t does not appear in Eq. (1).

EXACT OPEN-WALLED SECTION BEAM-THEORY EQUATIONS FOR M_{cr} – SINGLY-SYMMETRIC I-SECTION MEMBERS

A wide variety of different equations for the elastic LTB resistance have been considered in past research and Specification development activities. Many of the early developments are summarized by Clark and Hill (1960). These authors specify a general form for the theoretical elastic LTB resistance based on open-walled section beam theory, including the influence of cross-section monosymmetry, moment gradient, end-restraint conditions, and load height effects. (SSRC 1998) gives a general elastic LTB equation that is closely related to the one specified by Clark and Hill (1960), but in which the load height and moment gradient effects are handled with a single modification factor, denoted by the symbol C_b, and in which the monosymmetry characteristics are captured using a single parameter represented by the term β_x. For a general singly-symmetric member where the bending is in the plane of symmetry, the open-walled section beam theory solution for the elastic critical moment is expressed in (SSRC 1998) as

$$M_{cr} = F_{cr}S_{xc} = \frac{C_b \pi^2 EI_y}{2(K_y L_b)^2}\left\{\beta_x + \sqrt{\beta_x^2 + 4\left[\frac{C_w K_y^2}{I_y K_z^2} + \frac{GJ(K_y L_b)^2}{\pi^2 EI_y}\right]}\right\} \tag{7}$$

where β_x is the coefficient of monosymmetry (discussed below), and K_y and K_z are the effective length factors associated with end lateral and warping restraints respectively.

For a general singly-symmetric I-section as shown in Fig. 2, the key variables associated with Eq. (7) are as follows. The depth between the centroids of the flanges is expressed as

$$h = D + \frac{t_{ft} + t_{fc}}{2} \tag{8}$$

the distance from the centroid of the compression flange to the elastic neutral axis is

$$h_c = \frac{Dt_w(D + t_{fc})/2 + b_{ft}t_{ft}h}{b_{ft}t_{ft} + b_{fc}t_{fc} + Dt_w} \tag{9}$$

and the depth of the web in compression is

$$D_c = h_c - t_{fc}/2 \tag{10}$$

The term

$$y_o = -h_c + \alpha h \tag{11}$$

is the distance from the cross-section neutral axis to the shear center, negative if the larger flange is in compression, i.e., negative when the shear center lies between the centroid and the compression flange, as shown in Fig. 2. Also, the term α in Eq. (11) may be expressed as

$$\alpha = \frac{1}{1+\left(\frac{b_{fc}}{b_{ft}}\right)^3\left(\frac{t_{fc}}{t_{ft}}\right)} = \frac{1}{\frac{I_{yc}}{I_{yt}}+1} \tag{12}$$

where

$$I_{yc} = \frac{t_{fc} b_{fc}^3}{12}, \quad I_{yt} = \frac{t_{ft} b_{ft}^3}{12} \tag{13}$$

and the general warping constant for a singly-symmetric I-shape is given by

$$C_w = h^2 b_{fc}^3 t_{fc} \alpha / 12 = h^2 I_{yc} \alpha \tag{14}$$

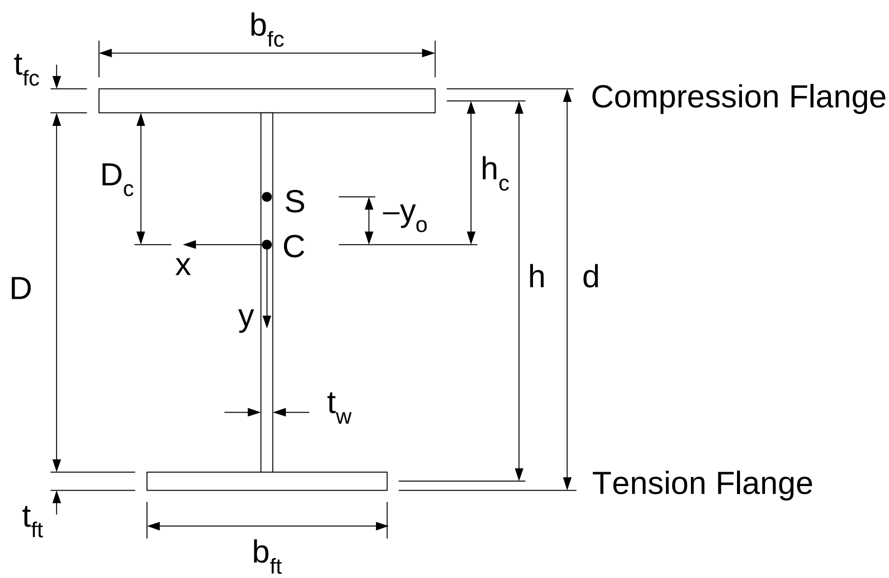

Figure 2. Cross-section dimensional terms for a singly-symmetric I-shape.

After h_c is determined using Eq. (9), the moment of inertia about the major-axis may be written as

$$I_x = b_{fc} t_{fc} h_c^2 + b_{ft} t_{ft} (h - h_c)^2 + D t_w (h_c - h/2)^2 + t_w D^3/12 + b_{fc} t_{fc}^3/12 + b_{ft} t_{ft}^3/12 \tag{15}$$

whereas the moment of inertia about the minor-axis is given by

$$I_y = I_{yc} + I_{yt} + D t_w^3/12 \tag{16}$$

The St. Venant torsion constant is expressed within the solutions considered in this paper as

$$J = \frac{Dt_w^3}{3} + \frac{b_{fc}t_{fc}^3}{3}\left(1 - 0.63\frac{t_{fc}}{b_{fc}}\right) + \frac{b_{ft}t_{ft}^3}{3}\left(1 - 0.63\frac{t_{ft}}{b_{ft}}\right) \tag{17}$$

The two bracketed terms within this equation account for the reduced torsional efficiency of stocky rectangular flanges relative to the ideal contribution $b_f t_f^3/3$. These terms give a highly accurate fit to refined solutions from elasticity theory, i.e., to solutions based on the membrane analogy. As can be observed from Eq. (17), the flange contributions are reduced relative to the ideal $b_f t_f^3/3$ values by more than 10 percent for sections with highly-stocky flanges. ElDarwish and Johnson (1965) suggest an equivalent expression to Eq. (17), but also provide a term that accounts for the beneficial "bubble" in the analogous membrane at the web-flange juncture, including the influence of web-to-flange fillets. The effect of this term is generally smaller than the bracketed terms in Eq. (17), and for sections with relatively thick flanges and thin webs, it is negligible.

The general equation for the coefficient of monosymmetry is defined as

$$\beta_x = \frac{1}{I_x}\int_A y\left(x^2 + y^2\right)dA - 2y_o \tag{18a}$$

If this equation is integrated exactly for a rectangular-flange I-shape, neglecting the web-flange weld geometry or fillets, β_x is obtained as

$$\begin{aligned}\beta_x = \frac{1}{I_x}\Bigg[&\left(\frac{b_{ft}^3}{12}(D - D_c)t_{ft} + \frac{b_{ft}^3}{24}t_{ft}^2 + b_{ft}t_{ft}(D - D_c)^3 + 1.5b_{ft}(D - D_c)^2 t_{ft}^2 + b_{ft}(D - D_c)t_{ft}^3 + \frac{b_{ft}}{4}t_{ft}^4\right) \\ &-\left(\frac{b_{fc}^3}{12}D_c t_{fc} + \frac{b_{fc}^3}{24}t_{fc}^2 + b_{fc}t_{fc}D_c^3 + 1.5b_{fc}D_c^2 t_{fc}^2 + b_{fc}D_c t_{fc}^3 + \frac{b_{fc}}{4}t_{fc}^4\right) \\ &+\left(\frac{(D - D_c)^4}{4}t_w + \frac{t_w^3}{24}(D - D_c)^2 - \frac{D_c^4}{4}t_w - \frac{t_w^3}{24}D_c^2\right)\Bigg] - 2y_o\end{aligned} \tag{18b}$$

(SSRC 1998) gives the following simplified form of this equation (after the correction of a minor typographical error):

$$\beta_x = \frac{1}{I_x}\left\{(h - h_c)\left[\frac{b_{ft}^3 t_{ft}}{12} + b_{ft}t_{ft}(h - h_c)^2 + \frac{t_w}{4}(h - h_c)^3\right] - h_c\left(\frac{b_{fc}^3 t_{fc}}{12} + b_{fc}t_{fc}h_c^2\right) - \frac{t_w h_c^4}{4}\right\} - 2y_o \tag{18c}$$

Also, (SSRC 1998) lists the following approximate equation for β_x from Kitipornchai and Trahair (1980):

$$\beta_x = 0.9h\left(\frac{2I_{yc}}{I_y} - 1\right)\left[1 - \left(\frac{I_y}{I_x}\right)^2\right] \tag{18d}$$

The Engineer should note that for this equation to correctly reduce to $\beta_x = 0$ in the limit that the cross-section is doubly-symmetric, I_y must be interpreted as $I_{yc} + I_{yt}$.

For typical beam-type I-sections (e.g., d/b_{fc} and d/b_{ft} both greater than about 1.7), the last bracketed term in Eq. (18d) is for all practical purposes equal to 1.0. Based on this assumption, and making the substitution $I_y = I_{yc} + I_{yt}$, Eq. (18d) can be written as

$$\beta_x = 0.9h\frac{\left(I_{yc}/I_{yt} - 1\right)}{\left(I_{yc}/I_{yt} + 1\right)} = 0.9h\alpha\left(\frac{I_{yc}}{I_{yt}} - 1\right) \tag{18e}$$

AS4100 (SAA 1998) suggests an equation that is equivalent to Eq. (18e) but with a constant of 0.8 instead of 0.9. The coefficient of 0.8 is based on the use of an assumed upper-bound value for I_y/I_x of 1/3, which is representative of column-type I-sections with a width of both flanges approximately equal to the section depth. For beam-type I-sections, I_y/I_x is typically on the order of 0.1 and Eq. (18e) is a better approximation. The specific nature of the approximation by Eq. (18e) is investigated for a wide range of I-sections subsequently in this paper.

SIMPLIFIED FORM OF THE EXACT OPEN-WALLED SECTION BEAM-THEORY EQUATIONS

The authors recommend the following based on the above developments. Engineers often consider it impractical to evaluate the effective length factors K_y and K_z in Eq. (7), and in many situations, the unbraced lengths are not sufficiently large to merit these calculations (i.e., the calculated inelastic LTB strengths are affected little by including K_y and K_z). Therefore, it is suggested that Eq. (7) should be expressed in the context of Specification provisions by replacing K_yL_b and K_zL_b with L_b. After substitution of $G = \frac{E}{2(1+\nu)} = \frac{E}{2.6}$ and some rearrangement of terms, Eq. (7) can be written in the form

$$M_{cr} = C_b\frac{\pi^2 EI_y}{L_b^2}\left\{\frac{\beta_x}{2} + \sqrt{\left(\frac{\beta_x}{2}\right)^2 + \frac{C_w}{I_y}\left[1 + 0.039\frac{J}{C_w}L_b^2\right]}\right\} \tag{19}$$

As noted previously for Eq. (7), this equation is a general form that is applicable for any singly-symmetric section bent about an axis perpendicular to the plane of symmetry.

The authors recommend the use of Eq. (18e) for hand-calculation of β_x, although the exact form of Eq. (18b) could certainly be programmed without difficulty. The errors associated with the use of Eq. (18e) are evaluated subsequently, and are found to be acceptable. Equations (14), (16), and (17) are recommended for the calculation of C_w, I_y and J respectively. It is suggested that Eq. (19) is simpler and more intuitive than the formula utilized in Appendix F1 of AISC (1999). The term $\frac{\pi^2 EI_y}{L_b^2}$ is of course the flexural buckling strength of the member as a column about the axis of symmetry, the term β_x gives a fundamental characterization of the lack of symmetry about the major-axis of bending, including the shift in the section shear center, the term $\frac{C_w}{I_y}$ can be interpreted as the ratio of the cross-section warping and minor-axis flexural bending efficiencies, and the product of the terms $\frac{C_w}{I_y}\frac{J}{C_w}=\frac{J}{I_y}$ is the ratio of the St. Venant torsion and minor-axis flexural bending efficiencies.

(SSRC 1998) recommends a useful design-based procedure for calculation of LTB effective length factors that accounts for the continuity with adjacent unbraced segments. This procedure is reasonably easy to apply, and in extraordinary circumstances (e.g., large unbraced lengths associated with elastic LTB during construction), it can give a substantially larger but typically conservative representation of the physical strength. This procedure was originally proposed by Nethercot and Trahair (1976), and involves the assumption that the lateral and warping restraints are identical and the calculation of an elastic effective length factor $K = K_y = K_z$ based on an analogy with the behavior of end-restrained columns. White and Chang (2005) present a generalization of the (SSRC 1998; Nethercot and Trahair 1976) procedure that addresses singly-symmetric I-shapes and composite I-sections in negative bending. If this or other procedures are used to calculate the LTB effective length factors, the term KL_b can be substituted for L_b in Eq. (19).

By equating Eq. (19) to the moment $M_{yr} = F_{yr}S_{xc}$ and taking $C_b = 1$ corresponding to the uniform bending case, this equation can be solved explicitly for the corresponding value of $L_b = L_r$. The resulting equation is first rewritten as an expression for L_r^2, which can be replaced conveniently by an arbitrary symbol, say X. The root of this quadratic equation is

$$X = L_r^2 = 0.192\pi^2\left(\frac{E}{F_{yr}}\right)^2\frac{I_yJ}{S_{xc}^2}\left\{\left[2.6\beta_x\frac{F_{yr}}{E}\frac{S_{xc}}{J}+1\right]+\sqrt{\left[2.6\beta_x\frac{F_{yr}}{E}\frac{S_{xc}}{J}+1\right]^2+27\frac{C_w}{I_y}\left(\frac{S_{xc}}{J}\right)^2\left(\frac{F_{yr}}{E}\right)^2}\right\} \tag{20}$$

which then gives

$$L_r = \frac{1.38}{S_{xc}}\frac{E}{F_{yr}}\sqrt{I_yJ}\sqrt{\left[2.6\beta_x\frac{F_{yr}}{E}\frac{S_{xc}}{J}+1\right]+\sqrt{\left[2.6\beta_x\frac{F_{yr}}{E}\frac{S_{xc}}{J}+1\right]^2+27\frac{C_w}{I_y}\left(\frac{F_{yr}}{E}\frac{S_{xc}}{J}\right)^2}} \tag{21}$$

Equation (21) is an exact closed-form equation for the noncompact bracing limit L_r (i.e., anchor point 2 of Fig. 1) based directly on open-walled section beam theory.

APPROXIMATION FOR M_{cr} IN AISC (1999)

When $K_y = K_z = K$, Eq. (7) also may be written as (Trahair 1977)

$$M_{cr} = \frac{\pi C_b}{KL_b}\left[\sqrt{EI_yGJ}\left(B_1+\sqrt{1+B_2+B_1^2}\right)\right] \tag{22}$$

where

$$B_1 = \frac{\pi \beta_x}{2(KL_b)}\sqrt{\frac{EI_y}{GJ}} \tag{23}$$

and

$$B_2 = \frac{\pi^2 EC_w}{(KL_b)^2 GJ} \tag{24}$$

Upon substituting Eq. (18e) for β_x, use of G = E/2.6 and assuming K = 1, Eq. (23) becomes

$$B_1 = 2.28\left[\frac{2I_{yc}}{I_y} - 1\right]\left(\frac{h}{L_b}\right)\sqrt{\frac{I_y}{J}} \tag{25}$$

This equation is specified in AISC (1999) with the exception that the coefficient of 2.28 is written as 2.25. Also, the Engineer should note that I_{yc}/I_y should be taken as $I_{yc}/(I_{yc} + I_{yt})$ for Eq. (22) to give the same result as Eqs. (1) and (2) in the limit that a section is doubly-symmetric.

Furthermore, by substituting Eq. (14) for C_w and by use of the approximation

$$\alpha = \frac{1}{1 + \frac{I_{yc}}{I_{yt}}} \cong \frac{1}{1 + \frac{I_{yc}}{(I_y - I_{yc})}} = \frac{I_y - I_{yc}}{I_y - I_{yc} + I_{yc}} = 1 - \frac{I_{yc}}{I_y} \tag{26}$$

Eq. (24) can be written as

$$B_2 = 25.7\left(1 - \frac{I_{yc}}{I_y}\right)\left(\frac{I_{yc}}{J}\right)\left(\frac{h}{L_b}\right)^2 \tag{27}$$

This equation is specified in AISC (1999) except that the coefficient of 25.7 is written as 25. Obviously, although the above expressions for B_1 and B_2 are appropriate algebraic simplifications, the physical significance of these terms within the context of Eq. (22) is somewhat difficult to understand. The authors prefer Eq. (19), which involves the direct use of the coefficient of monosymmetry β_x.

M_{cr} IN TERMS OF AN EQUIVALENT RADIUS OF GYRATION r_E

It is interesting to consider the equivalent radius of gyration obtained by equating the elastic buckling stress to Euler's column buckling equation (modified by C_b), i.e.,

$$F_{cr} = \frac{M_{cr}}{S_{xc}} = \frac{C_b}{S_{xc}} \frac{\pi^2 EI_y}{L_b^2}\left\{\frac{\beta_x}{2} + \sqrt{\left(\frac{\beta_x}{2}\right)^2 + \frac{C_w}{I_y}\left[1 + 0.0390\frac{J}{C_w}L_b^2\right]}\right\} = \frac{C_b \pi^2 E}{\left(\frac{L_b}{r_E}\right)^2} \tag{28}$$

If this equation is solved for r_E^2, the result is

$$r_E^2 = \frac{I_y}{S_{xc}} \left\{ \frac{\beta_x}{2} + \sqrt{\left(\frac{\beta_x}{2}\right)^2 + \frac{C_w}{I_y}\left[1 + 0.0390 \frac{J}{C_w} L_b^2\right]} \right\} \tag{29}$$

Based on this equivalent radius of gyration, the elastic critical moment may be expressed as

$$M_{cr} = \frac{C_b \pi^2 E}{\left(\frac{L_b}{r_E}\right)^2} S_{xc} \tag{30a}$$

or the elastic critical flange stress may be written as

$$F_{cr} = \frac{C_b \pi^2 E}{\left(\frac{L_b}{r_E}\right)^2} \tag{30b}$$

At first blush, this appears to be a dramatic simplification. However, this development is somewhat deceiving since the expression for r_E also contains the length L_b. The physical beam LTB behavior does not in general map all that well to the column elastic buckling equation. Therefore, the authors prefer the form given by Eq. (19).

GENERAL RELATIONSHIP BETWEEN r_E AND r_t

Equation (29) is useful for gaining a better understanding of several attributes of the elastic LTB equations. For instance, a common practice is to neglect the contribution from St. Venant torsion to the elastic LTB resistance in certain cases, or in other words, to assume $JL_b^2 = 0$ in determining the elastic LTB strength. This assumption is invoked commonly for slender-web I-girders, partly since flange raking and the associated web distortion are more likely as the web slenderness becomes large. Also, this assumption is often invoked in the development of equations for the length L_p corresponding to anchor point 1 in Fig. 1, since JL_b^2 in Eq. (28) becomes negligible for the short unsupported lengths associated with $L_b = L_p$ (White and Jung 2003a). By taking $JL_b^2 = 0$, Eq. (29) can be written as

$$r_{E(JL_b^2=0)}^2 = \frac{I_y}{S_{xc}} \left\{ \frac{\beta_x}{2} + \sqrt{\left(\frac{\beta_x}{2}\right)^2 + \frac{C_w}{I_y}} \right\} \tag{31}$$

In the limit that an I-shape becomes doubly symmetric, the monosymmetry parameter β_x approaches zero. Therefore, for the special case of a doubly-symmetric I-section, Eq. (31) reduces to

$$r^2_{E(JL_b^2=0,\, sym)} = \frac{\sqrt{C_w I_y}}{S_x} \tag{32}$$

White and Jung (2003a) show that this is the exact expression for r_t^2 in Eq. (2). That is, substitution of Eq. (32) for r_t^2 in Eq. (2) gives the exact solution for the elastic LTB resistance of a doubly-symmetric I-section member. Also, they show that Eq. (3) gives a close approximation of the exact r_t for doubly-symmetric I-shapes. In the context of this paper, it is important to note that Eq. (3) also gives an accurate approximation of $r_{E(JL_b^2=0)}$ from Eq. (31) for singly-symmetric I-sections. This result is demonstrated subsequently. Therefore, Eq. (3) may be used as an accurate general expression for r_t for all I-shapes. This result leads to the fact that Eqs. (2) and (5) can be applied with good accuracy to determine the elastic LTB strength for a wide range of singly-symmetric I-section members. Equation (32) is valid only for doubly-symmetric I-shapes and channels.

It is emphasized that for a doubly-symmetric I-section, $A_{wc} = D_c t_w = Dt_w/2$ in Eq. (3); however, for a singly-symmetric I-shape, $A_{wc} = D_c t_w \neq Dt_w/2$ in this equation. This extension of Eq. (3) is ad hoc. However, it works well as demonstrated in the following sections. Equation (3) is utilized for r_t to generate the results associated with Eq. (2) shown in this paper. Equation (3) simplifies to the traditional equation for the radius of gyration of the compression flange plus a third of the compressed portion of the web by taking D = h = d and neglecting the web-to-flange fillet areas, or if one considers that the product of the terms $\frac{D^2}{hd} < 1$ and $\left(1 + 6\frac{A_{fillet}}{A_{wc}}\right) > 1$ is approximately equal to one (White and Jung 2003a).

SPECIALIZATION OF THE EXACT OPEN-WALLED SECTION BEAM-THEORY EQUATIONS TO SLENDER WEB I-GIRDERS

If Eq. (19) is applied to slender-web I-sections, where J is taken equal to zero since significant flange raking and the associated web distortions are more likely, the elastic LTB strength simplifies to

$$M_{cr(J=0)} = C_b \frac{\pi^2 E I_y}{L_b^2}\left\{\frac{\beta_x}{2} + \sqrt{\left(\frac{\beta_x}{2}\right)^2 + \frac{C_w}{I_y}}\right\} \tag{33}$$

By recognizing the relationship for $r^2_{E(JL_b^2=0)}$ given by Eq. (31), Eq. (33) can be expressed in the form

$$F_{cr} = \frac{C_b \pi^2 E}{\left(\dfrac{L_b}{r_{E(JL_b^2=0)}}\right)^2} \tag{34}$$

In addition, based on the accurate approximation that Eq. (3) provides in general for $r_{E(JL_b^2=0)}$, this equation may be converted to

$$F_{cr} \cong \frac{C_b \pi^2 E}{\left(\frac{L_b}{r_t}\right)^2} \tag{35}$$

Also, the equivalent of Eq. (21) becomes

$$L_{r(J=0)} = \pi \sqrt{\frac{E}{F_{yr}} \frac{I_y}{S_{xc}} \left[\frac{\beta_x}{2} + \sqrt{\left(\frac{\beta_x}{2}\right)^2 + \frac{C_w}{I_y}} \right]} \tag{36}$$

or based on Eq. (31) and the observations discussed in the previous section,

$$L_{r(J=0)} = \pi r_{E(JL_b^2=0)} \sqrt{\frac{E}{F_{yr}}} \cong \pi r_t \sqrt{\frac{E}{F_{yr}}} \tag{37}$$

It can be observed that Eq. (35) takes the form of Euler's column buckling equation, modified by C_b, corresponding to an equivalent column composed of the compression flange plus a fraction of the compression area of the web. By calculating r_t including a portion of the web area, the effect of the web on the compression flange lateral stability is captured. In prior Specifications, it is not uncommon for Eq. (35) to be stated using the radius of gyration of the compression flange alone, r_{yc} (e.g., the elastic LTB strength of noncomposite slender-web I-girders is expressed in this fashion in AASHTO (1998)). It should be noted that if the radius of gyration of the compression flange alone ($r_{yc} = b_{fc}/\sqrt{12}$) is utilized in Eq. (35), the elastic LTB strength of the idealized girder (with J = 0) is generally overestimated. Furthermore, if r_{yc} is used in Eq. (35) instead of r_t, F_{cr} becomes independent of the proportions of the web and tension flange.

EVALUATION OF SIMPLIFIED LTB EQUATIONS FOR COMPACT AND NONCOMPACT-WEB I-SECTION MEMBERS VERSUS EXACT BEAM-THEORY

This section compares the results from the following elastic LTB expressions developed in the previous sections to the exact beam theory based solution from Eq. (19) with β_x given by the exact integration of Eq. (18a), i.e., using Eq. (18b):

1. The elastic LTB solution obtained using the rigorous Eq. (19), but with the simple approximate equation for β_x given by Eq. (18e),
2. The I_{yc}-based formula specified in AASHTO (1998), Eq. (1), and
3. The suggested r_t-based formula, Eq. (2), with r_t calculated using Eq. (3)[1].

All of the solutions within the parametric study are for the base case of uniform major axis bending, i.e., C_b = 1.0.

---

[1] All the calculations are conducted assuming welded I-sections; therefore, A_{fillet} is taken equal to zero.

Design of the Parametric Study

To compare the above equations in a reasonably comprehensive fashion while avoiding absurd or impractical cross-section geometries, the following ranges of the cross-section nondimensional variables are selected. The ratio of the web depth to the tension flange width is varied over the range

$1 \leq D/b_{ft} \leq 10$

and similarly, the range of the web depth to the compression flange width is taken as

$1 \leq D/b_{fc} \leq 6$

The value of one is considered to be a lower-bound practical limit for the above ratios, since for smaller values the corresponding flange is wider than the web is deep. The limit of $D/b_{fc} = 6$ is selected in the development of the updated AASHTO (2004) provisions based on the fact that the limited number of experimental tests with larger D/b_{fc} values tend to have a wide scatter in the measured strengths compared to predictions, with the measured strengths in a significant number of cases being quite low (White and Jung 2004; White and Kim 2004; White et al. 2004). The limit of $D/b_{ft} = 10$ is selected as a practical upper limit for the web depth to tension flange width based on judgment.

Also, bounds of one and six are established for the ranges of t_{fc}/t_w and t_{ft}/t_w, i.e.,

$1 \leq t_{fc}/t_w \leq 6$ and $1 \leq t_{ft}/t_w \leq 6$

and the upper bound for the web slenderness is taken as

$2D_c/t_w \leq 140$

The bound of $2D_c/t_w = 140$ is approximately the noncompact-web limit $5.7\sqrt{\frac{E}{F_y}}$ for $F_y = 50$ ksi (345 MPa) whereas the above restrictions on the flange-to-web thickness are considered as reasonable practical limits. That is, the web should not be thicker than the flanges and the flanges should not be excessively thick compared to the web. The value of six for the upper-bound on t_{fc}/t_w and t_{ft}/t_w corresponds to a hypothetical bridge I-girder with a 0.5 in (12.7 mm) thick web and a 3 in (76.2 mm) thick flange, or a 0.75 in (19.1 mm) thick web with a 4.5 in (114.3 mm) thick flange, or a hypothetical metal building I-section member with a 3/16 in (4.76 mm) web and a 1.125 in (28.6 mm) thick flange. Special considerations are typically necessary to weld flanges and webs that have this large of a disparity in their thicknesses. Also, sections with larger flange-to-web thickness ratios will tend to have slender webs. No limits are imposed on t_{fc}/t_w and t_{ft}/t_w in the subsequent slender-web member studies.

Within the above limits, all combinations and permutations of the following specific cross-section dimensional ratios are considered:

$b_{fc}/t_{fc} = 5, 10, 15$ and 24
$b_{ft}/t_{ft} = 5, 10, 15$ and 24
$D/b_{fc} = 1, 2, 3,$ and 6
$D/t_w = 5, 10, 40, 90, 140$ and 190

The smaller values of five for b_{fc}/t_{fc} and b_{ft}/t_{ft} are approximate lower-bound values for the flange total width-to-thickness ratios for rolled I-shapes (there are a few wide-flange sections that have b_f/t_f values between 3.6 and 5.0). Also, the smaller value of five for D/t_w is approximately a lower-bound of the web width-to-thickness ratio for rolled I-shapes (there a few wide-flange sections that have D/t_w values between 3.7 and 5.0). It is anticipated that engineers typically would not use plates that are this stocky for singly-symmetric I-section members, since it is likely that better economy can be obtained with more slender plates; nevertheless, these values are selected to test the limits of the suggested equations. The previously stated limits on D/b_{fc}, D/b_{ft}, t_{fc}/t_w, and t_{ft}/t_w often preclude the use of the smallest and largest D/t_w values listed above. In these cases, the bounds on D/t_w are established based on these limits. The value of $D/t_w = 190$ is selected as an upper-bound beyond which it is difficult to fabricate a singly-symmetric I-shape such that $2D_c/t_w \leq 140$. The largest value of b_{fc}/t_{fc} and $b_{ft}/t_{ft} = 24$ is the limit placed on the width-to-thickness of the flanges of I-shapes in AASHTO (1998 and 2004) to alleviate potential welding distortion problems.

For each specific combination of the dimensional ratios from the above lists, D/b_{ft} is varied to produce equal increments of $I_{yc}/(I_{yc} + I_{yt}) \cong 0.1$ within the above maximum and minimum limits on D/b_{ft}, D/b_{fc}, t_{fc}/t_w, t_{ft}/t_w and $2D_c/t_w$. Additional values of $I_{yc}/(I_{yc} + I_{yt})$ are considered for a number of the cross-sections that produce near maximum conservative or unconservative differences between the simplified equations and the exact beam theory solutions. The total number of cross-sections studied is 1630.

In addition to the above cross-section variables, the solutions are also a function of the unsupported length L_b. Based on the observation that the differences between the results of the simplified equations and the exact beam theory solutions vary in a monotonic fashion as a function of L_b, two values are considered for this parameter:

- $L_b = L_r$, and
- $L_b = \max(85b_{fc}, L_r)$

where L_r is calculated from Eq. (5) using $F_{yr} = 0.7F_y$ and $F_y = 50$ ksi (345 MPa). The value of $F_{yr} = 0.7F_y$ is specified in AASHTO (2004) and AISC (2005) for doubly-symmetric nonhybrid I-shapes, and is also applicable to singly-symmetric and hybrid I-sections in most cases. The yield strength is maintained at $F_y = 50$ ksi (345MPa) throughout the studies. The differences between the approximate and rigorous equations are generally smaller for larger yield strengths.

The length $L_b = L_r$ is the smallest value of L_b for which the elastic LTB equations are employed directly within the approach shown in Fig. 1. The length $L_b = 85b_{fc}$ is a practical upper-bound for the unbraced length. This value is suggested for the maximum length of a shipping piece in AASHTO (1998 and 2004). For a few of sections with $D/b_{fc} = 1$ and/or D/b_{ft} close to 1.0 and with stocky flanges, $85b_{fc}$ is smaller than L_r. In these cases, $L_b = L_r$ is used since L_r is the abscissa of anchor point 2 in Fig. 1. The L_r/r_t values range from 91 to 785, the L_r/b_{fc} values range from 18 to 155 and the L_r/D values range from three to 119 for the complete set of cross-sections considered. The $\max(85b_{fc}, L_r)/r_t$ values range from 276 to 785, the $\max(85b_{fc}, L_r)/b_{fc}$ values range from 85 to 155 and th $\max(85b_{fc}, L_r)/D$ values range from 14 to 119 for the complete set of cross-sections.

Discussion of Results

Figure 3 shows the ratio of the elastic LTB strengths obtained using the suggested exact form of the open-walled section beam theory equations, Eq. (19), with the simplified approximate expression for the cross-section monosymmetry parameter β_x given by Eq. (18e). The results in this figure are based on $L_b = L_r$. The error in the resulting solutions ranges from six percent unconservative to five percent conservative for $I_{yc}/(I_{yc} + I_{yt})$ ranging from 0.1 to 0.9. The accuracy for $L_b = \max(85b_{fc}, L_r)$ is better, with the largest errors relative to the exact beam theory solution being four percent unconservative to three percent conservative. Based on these results, it may be concluded that Eq. (18e) is an acceptable expression for β_x.

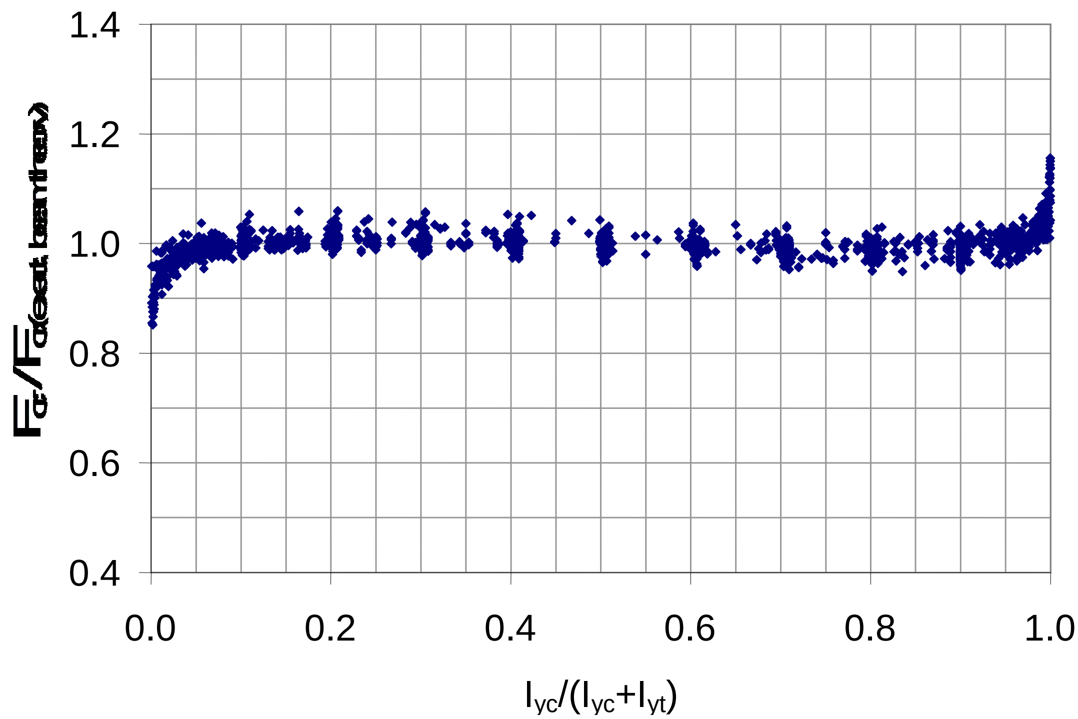

Figure 3. Ratio of the strength predicted by suggested form of the singly-symmetric LTB equation for F_{cr}, with Eq. (18e) used for β_x, to the exact beam theory elastic LTB solution, all compact- or noncompact-web sections with $L_b = L_r$, L_r based on $F_{yr} = 0.7F_y$ and $F_y = 50$ ksi (345 MPa), $C_b = 1$.

Figures 4 and 5 show the predictions by the AASHTO (1998) I_{yc}-based formula, Eq. (1), and by the suggested r_t-based formula, Eq. (2). These results are for $L_b = \max(85b_{fc}, L_r)$. If L_b is taken as L_r, the errors relative to the exact beam theory solutions are smaller. One can observe that the prediction of the exact beam theory strengths by these equations is in general rather poor. The errors associated with the I_{yc}-based formula range from 50 percent conservative to 27 percent unconservative whereas the r_t-based formula produces errors from 47 percent conservative to 20 percent unconservative for $I_{yc}/(I_{yc} + I_{yt})$ ranging from 0.1 to 0.9. Therefore, assuming that 20 or 27 percent unconservative error is unacceptable, it is clear that some restrictions on the use of these equations are necessary beyond the practical limits selected for the parametric study. The following general trends are evident in Figs. 4 and 5:

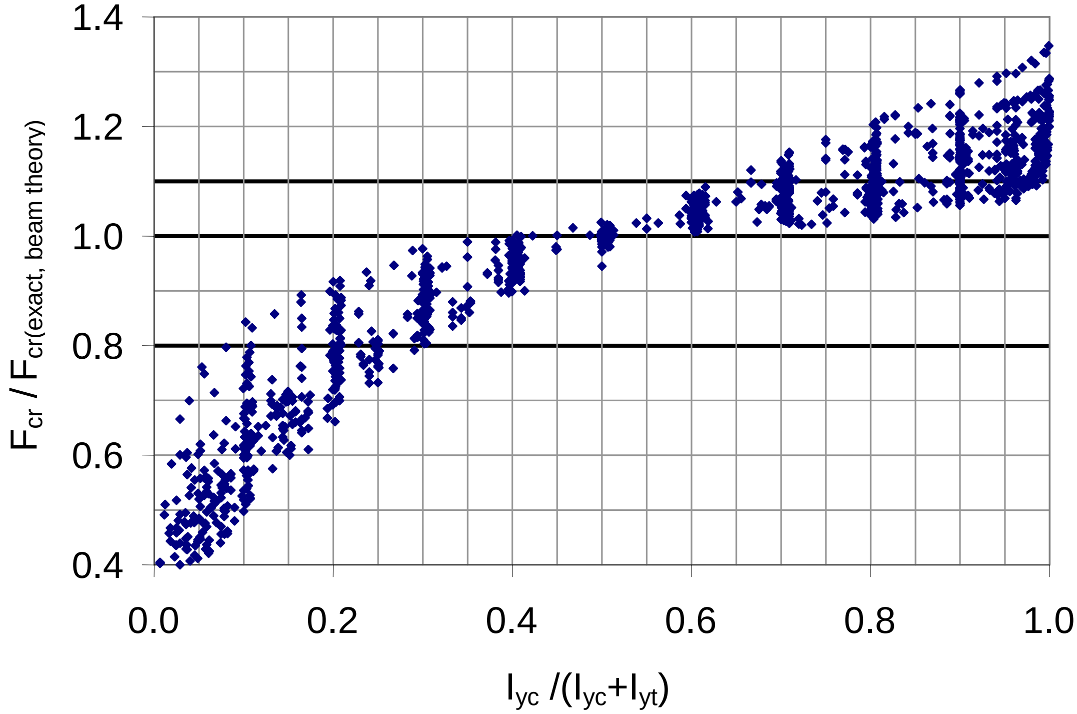

Figure 4. Ratio of strength predicted by I_{yc}-based LTB equation to the exact beam theory elastic LTB solution, all compact- or noncompact-web sections, $L_b = \max(85b_{fc}, L_r)$, L_r based on $F_{yr} = 0.7F_y$ and $F_y = 50$ ksi (345 MPa), $C_b = 1$.

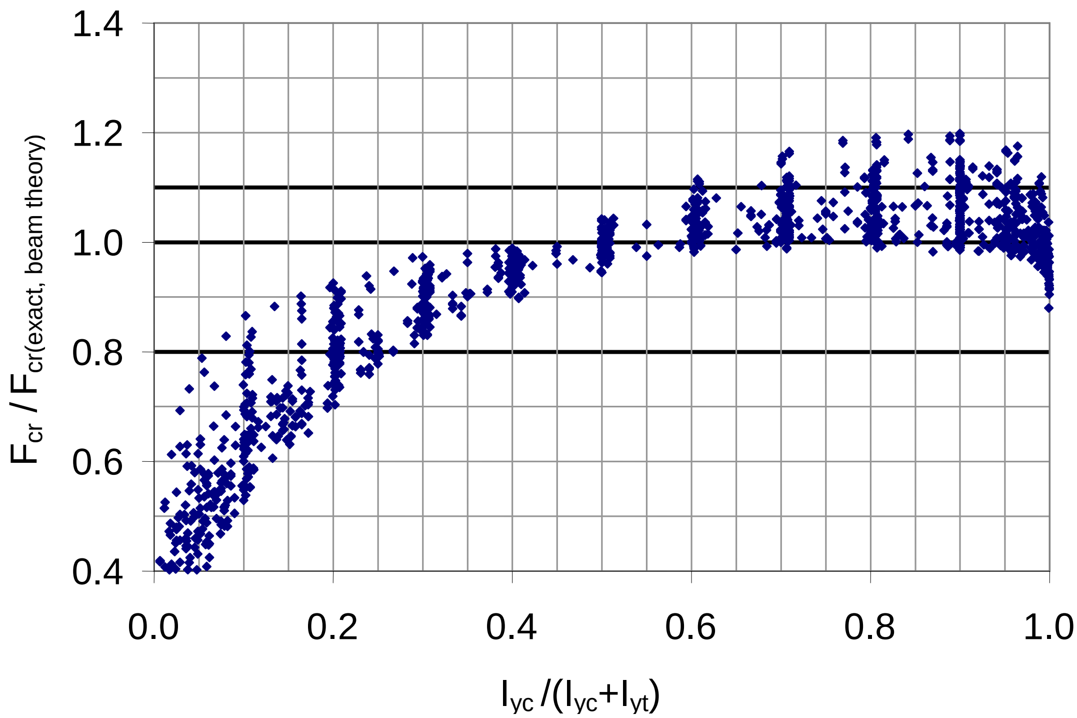

Figure 5. Ratio of strength predicted by r_t-based LTB equation to the exact beam theory elastic LTB solution, all compact- or noncompact-web sections, $L_b = \max(85b_{fc}, L_r)$, L_r based on $F_{yr} = 0.7F_y$ and $F_y = 50$ ksi (345 MPa), $C_b = 1$.

- The doubly-symmetric equations tend to give their most unconservative predictions relative to the exact beam theory results at large $I_{yc}/(I_{yc} + I_{yt})$, i.e., for cross-sections with a larger compression flange. If 10 percent unconservative error relative to the exact beam theory solution is selected as a maximum acceptable limit, the use of Eqs. (1) and (2) must be restricted in general to $I_{yc}/(I_{yc} + I_{yt}) \leq 0.6$ (i.e., $I_{yc}/I_{yt} \leq 1.5$).
- The doubly-symmetric equations tend to be most conservative relative to the exact beam theory solution for small $I_{yc}/(I_{yc} + I_{yt})$, i.e., for cross-sections with the smaller flange in compression. If 20 percent conservative error is selected as a maximum acceptable limit, the use of Eqs. (1) and (2) must be restricted in general to $I_{yc}/(I_{yc} + I_{yt}) \geq 0.3$ (i.e., $I_{yc}/I_{yt} = 0.43$).

The largest errors in Eqs. (1) and (2) with respect to the exact beam theory solution occur for shallow-depth members (small D/b_f) with stocky plate elements (small b_{fc}/t_{fc}, b_{ft}/t_{ft} and D/t_w). Figures 6 and 7 show the results at $L_b = L_r$ if the minimum D/b_{fc} and D/b_{ft} values are limited to two, and the minimum width-to-thickness ratio of the tension flange is limited to $b_{ft}/t_{ft} = 10$ (i.e., $b_{ft}/2t_{ft} \geq 5$). These restrictions are believed to be practical for a large number of bridge I-girders as well as singly-symmetric I-section members used in steel building construction. Given these restrictions, the I_{yc}-based formula ranges from 16 percent conservative to 14 percent unconservative for $0.1 \leq I_{yc}/(I_{yc} + I_{yt}) \leq 0.9$. However, the suggested r_t-based equation (Eq. (2)) gives errors that are only a maximum of two percent unconservative to 12 percent conservative relative to the exact beam theory results.

The errors relative to the exact beam theory solution are somewhat larger if plots comparable to Figs. 6 and 7 are considered but with $L_b = \max(85b_{fc}, L_r)$ (not shown). In this case, the errors in the I_{yc} formula range from -37 to +21 percent, with the positive sign indicating an over-prediction of the theoretical results. However, the r_t-based formula gives errors from -35 to only +9 percent. Given the tendency of web distortion to reduce the strength of members with the smaller flange in compression, the conservative nature of the r_t formula for small $I_{yc}/(I_{yc} + I_{yt})$ is considered to be acceptable. The reduction in the LTB strength due to web distortion is addressed by White and Jung (2003b).

Figure 8 is a repeat of Fig. 5 in which J is reduced by 20 percent for I-shapes with $I_{yc}/I_{yt} > 1.5$ whenever $D/b_{fc} < 2$, $D/b_{ft} < 2$, or $b_{ft}/t_{ft} < 10$. The resulting maximum unconservative error relative to the exact beam theory strengths is nine percent. Although the above reduction in J results in a discontinuity in the predicted strengths at $I_{yc}/I_{yt} = 1.5$, this discontinuity is within the range of the errors exhibited by the r_t-based equation relative to the exact beam theory solutions.

Lastly, Fig. 9 shows the correlation between r_t given by Eq. (3) and $r^2_{E(JL_b^2=0)}$ given by Eq. (31). The maximum unconservative difference between these two variables is four percent and the maximum conservative difference is 14 percent for $I_{yc}/(I_{yc} + I_{yt})$ from 0.1 to 0.9.

COMPARISON OF FORMULAE BASED ON J = 0

This section compares the results from the suggested r_t-based equation to the results from the direct open-walled section beam theory solution when the St. Venant torsional constant is taken equal to zero, i.e., Eq. (4) versus Eq. (33). The same limits on the cross-section parameters are employed in this study as in the previous one, except that $2D_c/t_w$ is limited to a maximum of 280 and a minimum of 90, specific values of 90, 140 and 280 are specified for D/t_w, and no maximum limits are placed on t_{fc}/t_w and t_{ft}/t_w. The value of $2D_c/t_w = 280$ is close to the

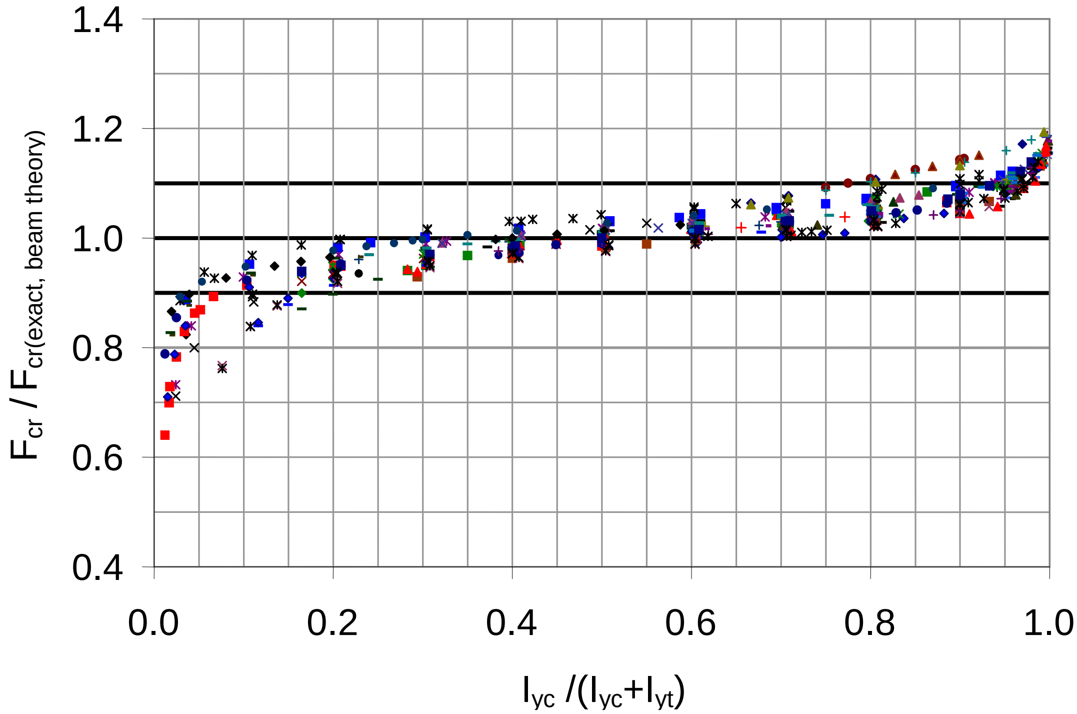

Figure 6. Ratio of strength predicted by I_{yc}-based LTB equation to the exact beam theory elastic LTB solution, compact- and noncompact-web sections with $D/b_{fc} \geq 2$, $D/b_{ft} \geq 2$ and $b_{ft}/t_{ft} \geq 10$, $L_b = L_r$, L_r based on $F_{yr} = 0.7F_y$ and $F_y = 50$ ksi (345 MPa), $C_b = 1$.

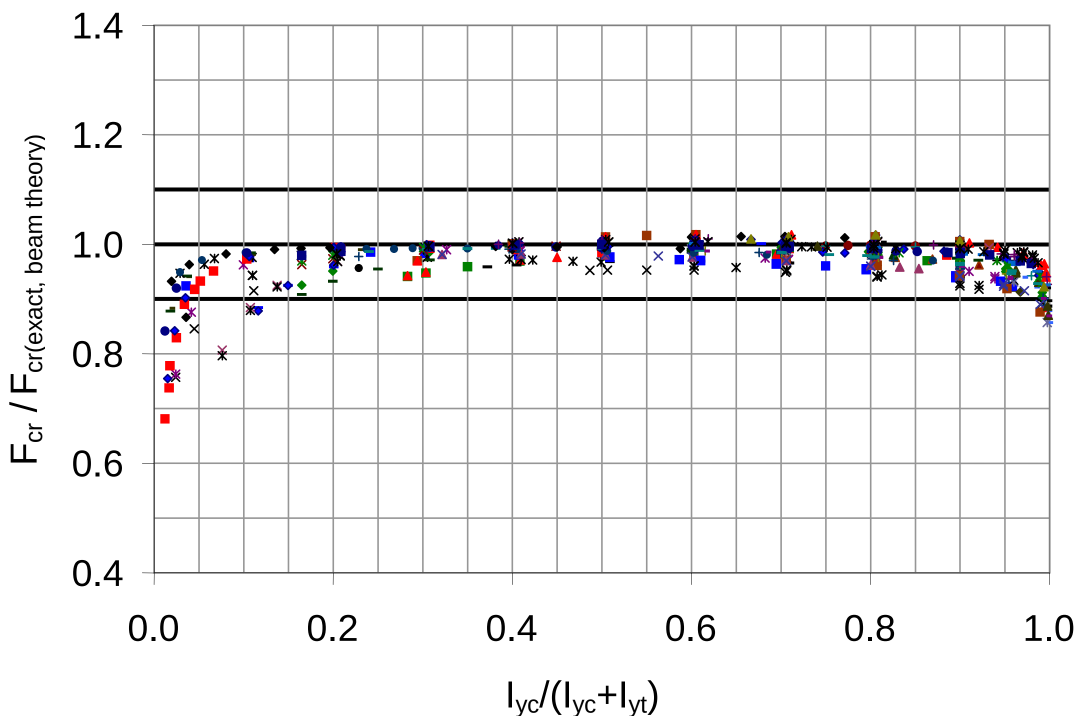

Figure 7. Ratio of strength predicted by r_t-based LTB equation to the exact beam theory elastic LTB solution, compact- and noncompact-web sections with $D/b_{fc} \geq 2$, $D/b_{ft} \geq 2$ and $b_{ft}/t_{ft} \geq 10$, $L_b = L_r$, L_r based on $F_{yr} = 0.7F_y$ and $F_y = 50$ ksi (345 MPa), $C_b = 1$.

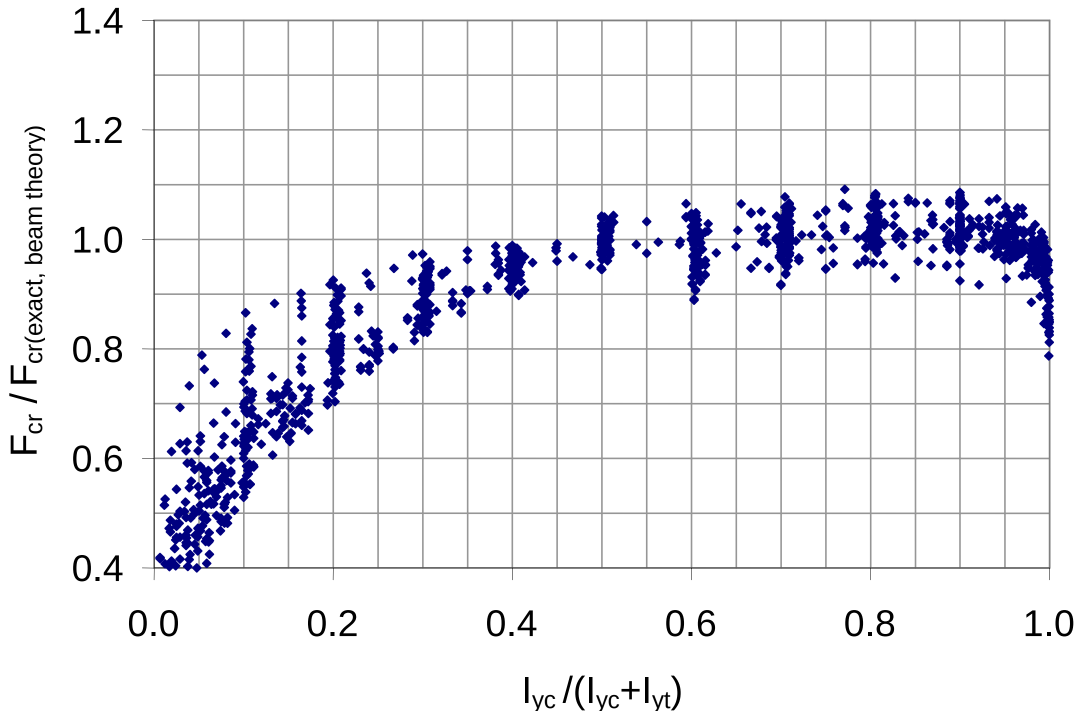

Figure 8. Ratio of strength predicted by r_t-based LTB equation (with J multiplied by 0.8 for sections with $D/b_{ft} < 2$, $D/b_{fc} < 2$ or $b_{ft}/t_{ft} < 10$) to the exact beam theory elastic LTB solution, all compact- or noncompact-web sections, $L_b = \max(85b_{fc}, L_r)$, L_r based on $F_{yr} = 0.7F_y$ and $F_y = 50$ ksi (345 MPa), $C_b = 1$.

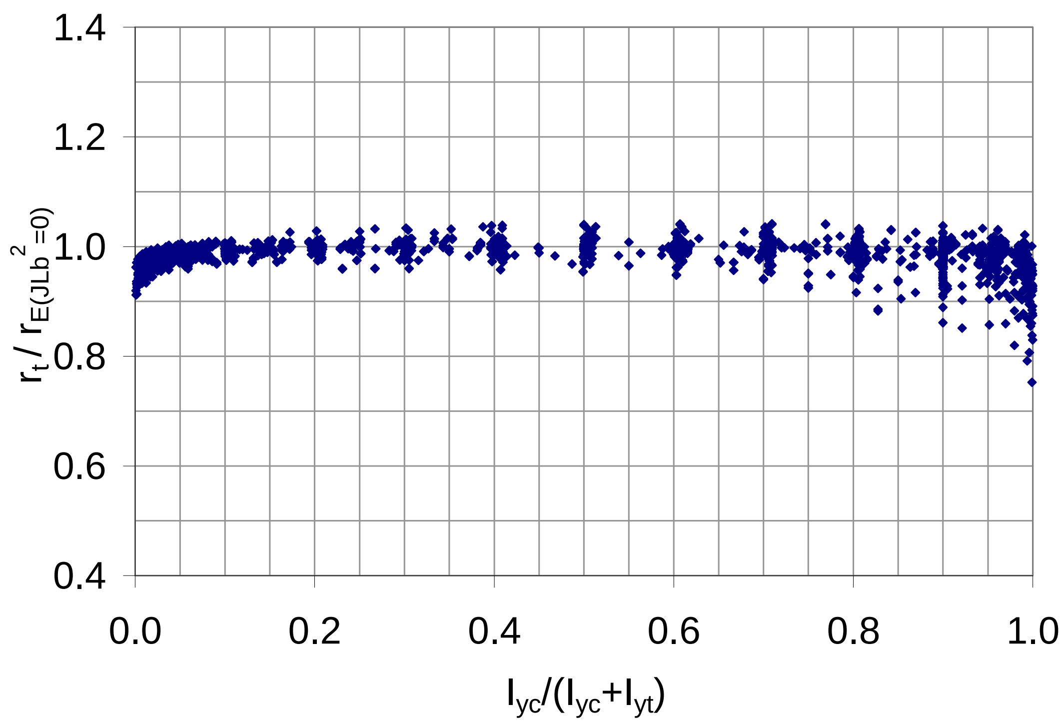

Figure 9. Ratio of r_t to $r_{E(JL_b^2=0)}$, all compact- and noncompact-web sections.

maximum value allowed for longitudinally-stiffened I-girders in AASHTO (2004) and D/t_w = 280 is approximately the maximum limit allowed in AISC (1999 and 2005) for slender-web I-girders with closely-spaced transverse stiffeners and F_y = 50 ksi (345 MPa). The minimum $2D_c/t_w$ of 90 is slightly less than the noncompact-web limit $5.7\sqrt{\frac{E}{F_y}}$ for F_y = 100 ksi (690 MPa). The total number of cross-sections considered is 1305. The comparison of the above two equations is independent of L_b; therefore, a specific unbraced length does not need to be defined.

Figure 10 summarizes the results for this parametric study. One can observe that for $I_{yc}/(I_{yc} + I_{yt})$ between 0.1 and 0.9, the ratio of the results obtained by Eq. (4) versus Eq. (33) ranges from 15 percent conservative to nine percent unconservative. Since Eqs. (4) and (33) are proportional to r_t^2 and $r^2_{E(JL_b^2=0)}$ respectively, Fig. 10 is also a plot of $r_t^2 / r^2_{E(JL_b^2=0)}$. As explained by White and Jung (2003b), the LTB solutions using J = 0 are generally conservative for compact- and noncompact-web members relative to distortional buckling solutions, although in some cases, this conservatism is minor. This behavior is expected in general also for slender-web members; however, the solutions based on J = 0 are expected to give only minor conservative error in many cases. White and Jung (2004) show that the predictions of slender-web member experimental inelastic and elastic LTB strengths using Eq. (4) as the base elastic LTB resistance are quite good, with the results being slightly more conservative overall for members with unbraced lengths approaching or exceeding L_r.

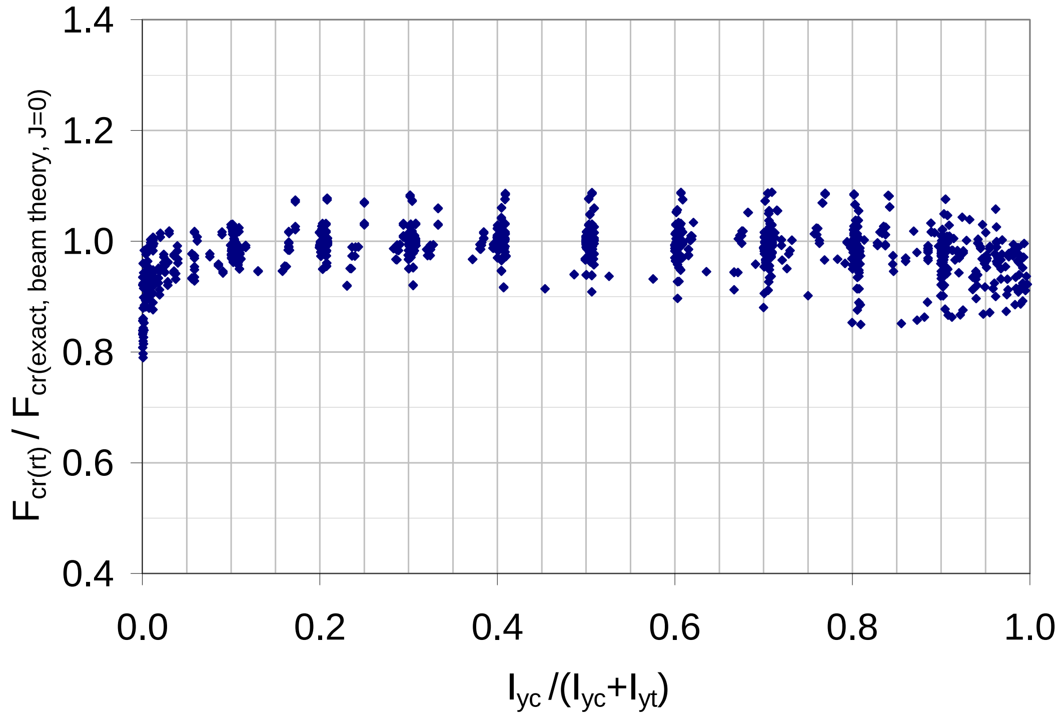

Figure 10. Ratio of strength predicted by r_t-based LTB equation (Eq. (4)) to the exact beam theory elastic LTB solution with J taken equal to zero (Eq. (33)), all slender-web sections (C_b = 1).

APPLICATION OF EQUATIONS TO COMPOSITE I-SECTIONS IN NEGATIVE BENDING AND TO CHANNEL-CAPPED I-SECTIONS

The application of the rigorous open-walled section beam theory equations to composite I-sections in negative bending is difficult. Because of the lateral rigidity of the slab, the shear center of the composite section will be near the slab centroid, the term α (Eq. (12)) will be close to one, and the coefficient of monosymmetry β_x will be approximately equal to $-h$ based on the approximate Eq. (18e). Furthermore, the application of Eq. (19) is questionable because of the large I_y and J contributions from the slab. The key problem here is that the lateral buckling of the bottom flange involves distortion of the web whereas the beam theory equations in turn assume that the web does not distort, i.e, they are based on the assumption that the I-section profile is effectively rigid.

Oehlers and Bradford (1995 and 1999) provide an extensive discussion and review of research relevant to the general distortional bucklng problem as well as research specifically relevant to the distorsional buckling problem in composite beams. They recommend an "inverted U-frame" approach for determination of the elastic distortional buckling moment. This moment is then used within an ultimate strength curve to determine the design capacity, similar to the approach recommended by Schaffer (2003) for handling of distortional buckling in cold-formed steel members. The U-frame model entails the idealization of the compression flange as an elastic column on an elastic foundation (the web) subjected to uniform compression. The conservatism of this model is acknowledged by Oehlers and Bradford. Kemp (1996) and Dekker et al. (1995) also discuss the composite beam distortional buckling problem, and suggest a single effective length factor of 0.71 that they use in the context of specialized strength equations directed at capturing the interaction between local and lateral buckling.

The r_t-based LTB equations, Eqs. (2), (3) and (5), combined with the unified flexural resistance provisions for I-section members in AASHTO (2004) and AISC (2005), provide a conservative but practical and sufficient solution for the LTB strength of many practical composite I-section members in negative bending. In this approach, the r_t parameter (Eq. (3)) is calculated based on the depth of the web in compression within the composite member, the contribution of the slab to the St. Venant torsion constant J is neglected (J is calculated based on the steel I-section using Eq. (17)), and the section modulus S_{xc} is calculated as M_{yc}/F_{yc} where M_{yc} is the yield moment of the cross-section determined considering the noncomposite and composite loadings using the procedures in AASHTO (1998 and 2004). The reader is referred to White (2004) for a detailed technical overview of the I-section member unified flexural resistance provisions of the above Specifications.

A number of prior research studies have shown that it is generally conservative to test the stability behavior of composite beams in negative bending by using a large steel tension flange, or a cover-plated flange. These elements provide a force equivalent to that developed by the slab within the prototype composite member (Barth and White, 1997; White and Barth 1998; Kemp 1996; Grubb and Carskaddan 1981 and 1979, Climenhaga and Johnson 1972). The results in this paper show that Eqs. (2) and (3) give conservative predictions of the elastic LTB strengths for a wide range of all-steel singly-symmetric members. In the extreme cases where these equations give unconservative predictions, the unconservative error is more than compensated for if a representative estimate of the lateral and torsional restraint from the slab is included within the FEA distortional buckling models. Therefore, it can be stated that the use of Eqs. (2), (3) and (5) is generally conservative for composite I-beams and I-girders both in building and in bridge construction. This solution is sufficient since, once the C_b parameter is included to account for moment gradient effects typical of negative moment regions, the member strengths tend to be at or close to M_{max} in Fig. 1 for practical brace spacings.

As an illustration, the Engineer is referred to the shored composite beam analyzed in Examples 13.1 and 13.2 of Oehlers and Bradford (1999) and shown in Fig. 11. The plastic moment capacity of this composite beam, using the procedures in AISC (1999 and 2005) and AASHTO (1998 and 2004), is 332 kNm (245 ft-k). The unbraced length L_b specified by Oehlers and Bradford is 7 m (23.0 ft), which is greater than L_r from Eq. (5). Oehlers and Bradford give three different estimates of the capacity of this beam: M_n/M_p = 0.728, 0.946, and 1.08. The later two strengths are obtained by first calculating a flexural capacity of the steel section alone, then adding a couple associated with the tension in the slab reinforcing steel to the steel section flexural capacity. No reduction is taken in the flexural resistance of the steel section due to this axial force however. This leads to an over-estimation of the composite beam strength particularly in the last case, where the steel section is already at its plastic moment prior to adding the couple associated with the slab force. Based on the procedures in AASHTO (2004), which use Eq. (2) for the elastic LTB strength, M_n/M_p = 0.356 for C_b = 1 while M_n/M_p = 0.819 for C_b = 2.3. Practically speaking, L_b = 7 m is not a realistic unbraced length for this cross-section. Since L_b/D is 23.3, L_b = 7 m is more representative of an entire span length. Suppose that the span length of this beam is 7 m (23.0 ft) and the member is braced laterally at its ends and at its midspan. In this case, 2.3 is a likely potential value for C_b, and the procedures in AASHTO (2004) give $M_n = M_p$.

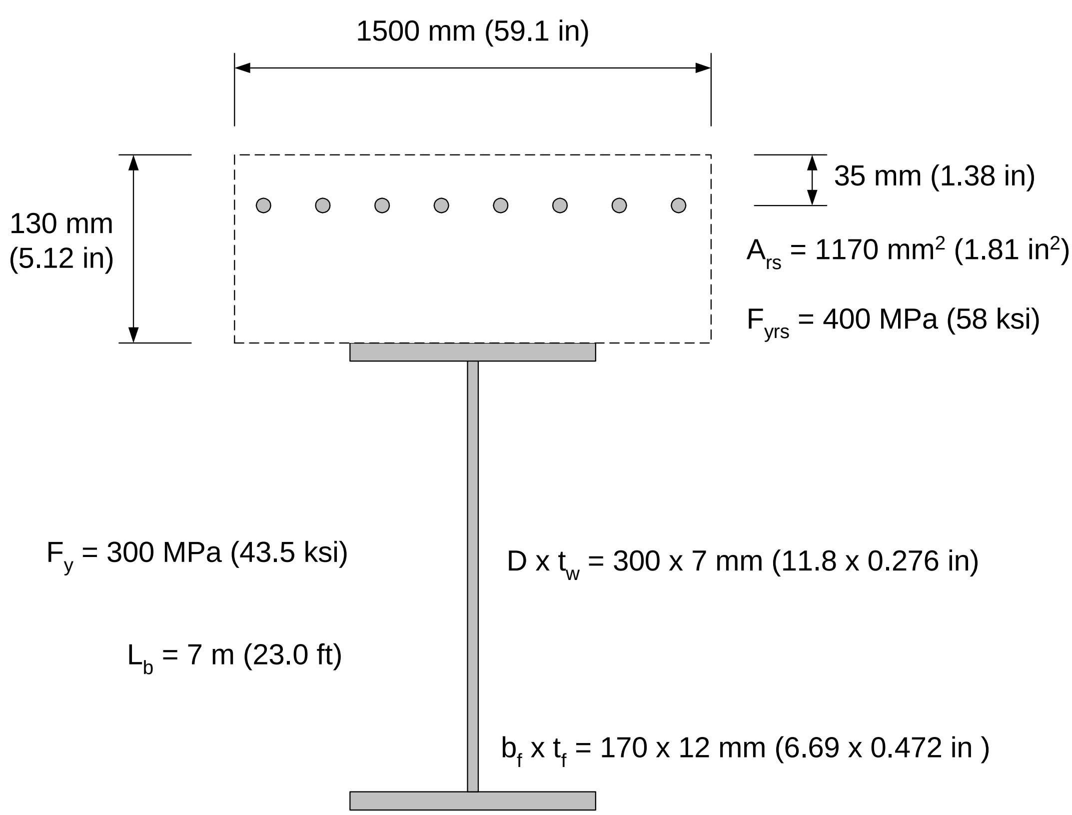

Figure 11. Composite beam in negative bending studied by Oehlers and Bradford (1999).

Application of the suggested rigorous beam theory equations to capped channel sections is relatively straightforward since Eq. (19) applies generally to the major-axis bending of any type of singly-symmetric cross-section. The key differences relative to the solutions for rectangular-flange I-shapes discussed within the previous sections are in the determination of I_y, β_x, C_w and J. The lateral moment of inertia I_y is calculated simply as the sum of the corresponding moments of inertia from the I-shape and from the channel cap. The coefficient of monosymmetry β_x is obtained directly from Eq. (18a). Lue and Ellifritt (2003) discuss the calculation of C_w for these types of sections. Their procedure amounts to a subdivision of the cross-section into various rectangular areas, with the channel web and the I-shape flange grouped together where they are in contact. The St. Venant torsional constant J is determined conservatively by summing the J values from the channel and from the I-shape, i.e., neglecting the influence of the interconnection of these shapes on the stresses and strains associated with uniform torsion.

The r_t-based equation also can be applied to determine the elastic LTB strength of a channel-capped I-section. In this case, the radius of gyration r_t is taken as that of the channel + the flange of the I-girder + 1/3 of the area of the web of the I-shape in compression. As suggested above, J is determined by summing the St. Venant torsional constants from each of the shapes. The elastic section modulus S_{xc} is calculated as I_x/y_{top} based on elementary strength of materials concepts, where y_{top} is the distance from the centroid of the full cross-section to the extreme fiber of the channel cap. Finally, the parameter h is taken as the distance between the centroid of the compression flange plus the channel cap to the mid-thickness of the bottom flange. The resulting elastic LTB strengths are comparable to those obtained using the rigorous beam theory equations.

As an illustration, consider the calculation of L_r for a W36x150 with a C15x33.9 channel cap. Lue and Ellifritt (2003) determine C_w = 132100 in^6 (35.48x10^{12} mm^6) for this combined section. The shear center is located at y_o = -6.79 in from the section centroid (Lue and Ellifritt 2003). The coefficient of monosymmetry β_x evaluates to 18.75 in (476.2 mm) using Eq. (18a). All of the other cross-section parameters are readily available or are easily calculated. Based on $F_{yr} = 0.7F_y$ and F_y = 50 ksi (345 MPa), L_r evaluates to 439.4 in (11,160 mm) from Eq. (21). Correspondingly, if Eq. (5) is used to calculate L_r, the depth of the web in compression is first calculated as D_c = 13.76 in (349.5 mm), r_t evaluates to 4.333 in (110.1 mm), and h is obtained as 35.50 in (901.7 mm). Equation (5) then gives L_r = 418.5 in (10,630 mm), which is 95 percent of the L_r obtained from the rigorous beam theory equations. Furthermore, F_{cr} based on Eq. (2) evaluates to 32.08 ksi (221.2 MPa) or 0.917 F_{yr} = 0.642 F_y at $L_b = L_r$ = 439.4 in (11,160 mm) from the rigorous beam theory equations.

SUMMARY

Based on the results presented in this study, the following elastic LTB equations are recommended:

1. For all I-section members with slender webs (composite in negative bending and noncomposite), Eq. (4) for F_{cr} and Eq. (6) for L_r, with r_t calculated using Eq. (3) for members with a rectangular compression flange. For these types of members with built-up compression flanges or with channel caps, r_t may be calculated as the radius of gyration about the plane of the web for the flange components plus one-third of the area of the web in flexural compression.

2. For compact- and noncompact-web composite I-sections in negative bending, Eq. (2) for F_{cr} and Eq. (5) for L_r, with r_t calculated using Eq. (3) for members with rectangular compression flanges. For these types of members with built-up compression flanges (e.g., cover-plated flanges), r_t may be calculated as the radius of gyration about the plane of the web for the flange components plus one-third of the area of the web in flexural compression.
3. For compact- and noncompact-web doubly-symmetric I-section members, Eq. (2) for F_{cr} and Eq. (5) for L_r, with r_t calculated using Eq. (3) for members with rectangular compression flanges (an alternative exact form for r_t in these cases is presented by White and Jung (2003a)). For these types of members with built-up compression flanges, r_t may be calculated as the radius of gyration about the plane of the web for the flange components plus one-third of the area of the web in flexural compression, which is one-sixth of the total area of the web.
4. For compact- and noncompact-web singly-symmetric noncomposite I-section members, either of the following alternative equations:
    a. Eq. (2) for F_{cr} and Eq. (5) for L_r, with r_t calculated using Eq. (3) for members with rectangular compression flanges. For these types of members with built-up compression flanges or with channel caps, r_t may be calculated as the radius of gyration about the plane of the web for the flange components plus one-third of the area of the web in flexural compression.
    b. Eq. (19) for M_{cr} and Eq. (21) for L_r, with β_x calculated using Eq. (18e) and C_w computed using Eq. (14) for members with rectangular flanges. For general members, β_x should be calculated using Eq. (18a) and C_w should be calculated from the fundamental principles of open-walled section beam theory on which these equations are based.

The authors prefer Eqs. (2) and (5) as a simple set of equations that give accurate to somewhat conservative solutions for the second, third and fourth of the above groups, within the context of the restrictions stated below. These equations have the advantage that the buckling moment M_{cr} depends only on basic and relatively easily understood parameters C_b, S_{xc}, $\frac{L_b}{r_t}$, and $\frac{S_{xc}h}{J}$, and the noncompact bracing limit depends only on r_t, $\frac{E}{F_{yr}}$, and $\frac{S_{xc}h}{J}$. Furthermore, Eqs. (2) and (5) reduce to the established forms for M_{cr} and L_r for slender-web members simply by setting $J = 0$ within Eq. (2). More accurate beam theory results are obtained using Eqs. (19), (21) and (18e), but for highly singly-symmetric-members with a smaller flange in compression, the applicability of these equations, as well as Eqs. (2) and (5), is limited in general due to web distortion (White and Jung 2003b). Equation (2) tends to give solutions that are more conservative than the rigorous beam theory Eq. (19) in these cases. However, the approximation of the rigorous beam theory solution by Eq. (2) is highly accurate for members with $D/b_{ft} \geq 2$, $D/b_{fc} \geq 2$ and $b_{ft}/t_{ft} \geq 10$ (see Fig. 7).

The St. Venant torsional constant should be calculated using Eq. (17) in general in all of the approaches, or the more exact version of this equation that includes the bubble in the analogous membrane at the web flange juncture forwarded by ElDarwish and Johnston (1965) should be employed. The use of the ideal $b_f t_f^3/3$ contribution from the flanges overestimates the actual value of J by a significant percentage for members with stocky flanges.

If Eqs. (2) and (5) are used for members within the fourth of the above groups, the above St. Venant torsional constant J should be multiplied by 0.8 whenever I_{yc}/I_{yt} is greater than 1.5, unless $D/b_{ft} \geq 2$, $D/b_{fc} \geq 2$ and $b_{ft}/t_{ft} \geq 10$. This factor is required in these cases to limit the unconservative error associated with the use of Eq. (2) to a maximum of 9 percent for stocky column-type cross-sections that are singly-symmetric.

The influence of web distortion on the LTB strength, and the corresponding implications relative to the use of beam-theory based formulae, are addressed by White and Jung (2003b).

ACKNOWLEDGEMENTS

This work was funded by Professional Services Industries, Inc. (PSI) and the Federal Highway Administration (FHWA). The financial support from these organizations is gratefully acknowledged. The opinions, findings and conclusions expressed in this paper are the authors' and do not necessarily reflect the views of the above organizations

REFERENCES

AASHTO (2004). *AASHTO LRFD Bridge Design Specfciations, 3rd Edition*, American Association of State and Highway Transportation Officials, Washington, D.C.

AASHTO (1998). *AASHTO LRFD Bridge Design Specifications 2nd Edition with 1999, 2000 and 2001 Interims*, American Association of State and Highway Transportation Officials, Washington D.C.

AISC (2005). *Specification for Structural Steel Buildings*, American Institute of Steel Construction, Chicago, IL (to appear).

AISC (1999). *Load and Resistance Factor Design Specification for Structural Steel Buildings*, American Institute of Steel Construction, Chicago, IL, 292 pp.

Barth, K. E., and White, D. W. (1997). "Finite Element Evaluation of Pier Moment-Rotation Characteristics in Continuous-Span Steel I-Girders." *Engineering Structures*, 20(8), 761-778.

Clark, J.W. and Hill, H.N. (1960). "Lateral Buckling of Beams," *Journal of the Structural Division*, ASCE, 86(ST7), 175-196.

Climenhaga, J.J. and Johnson, R.P. (1972). "Local buckling in continuous composite beams," *The Structural Engineer,"* 50(9), 367-374.

Dekker, N.W., Kemp, A.R. and Trinchero, P. (1995). "Factors Influencing the Strength of Continuous Composite Beams in Negative Bending," *Journal of Constructional Steel Research*, 34(2-3), 161-186.

ElDarwish, I.A. and Johnston, B.G. (1965). "Torsion of Structural Shapes," *Journal of the Structural Division*, ASCE, 91(ST1), 429-453.

Grubb, M. A., and Carskaddan, P. S. (1981). *Autostress design of highway bridges, phase 3: Moment rotation requirements.*, Research Laboratory Rep., United States Steel Corporation, Monroeville, PA.

Grubb, M. A., and Carskaddan, P. S. (1979). *Autostress design of highway bridges, phase 3: Initial moment rotation tests.*, Research Laboratory Rep., United States Steel Corporation, Monroeville, PA.

Kemp, A.R. (1996). “Inelastic Local and Lateral Buckling in Design Codes,” *Journal of Structural Engineering*, 122(4), 374-381.

Kitipornchai, S. and Trahair, N.E. (1980). “Buckling Properties of Monosymmetric I-Beams,” *Journal of the Structural Division*, ASCE, 106(ST5), 941-958.

Lue, D.M. and Ellifritt, D.S. (2003). ”Numerical Evaluation for Warping Constant of Built-Up Crane Runway Beam,” *Proceedings*, Structural Stability Research Council, Annual Technical Session and Meeting, Univ. Missouri, Rolla, MO., 213-232.

Nethercot, D.A and Trahair, N.S. (1976). “Lateral Buckling Approximations for Elastic Beams,” *The Structural Engineer*, 54(6), 197-204.

Oehlers, D.J. and Bradford, M.A. (1999). *Elementary Behavior of Composite Steel and Concrete Structural Members*, Butterworth Heinemann, Oxford, 259 pp.

Oehlers, D.J. and Bradford, M.A. (1995). *Composite Steel and Concrete Structural Members*, Fundamental Behavior, Elsevier, NY, 549 pp.

SAA (1998). *Steel Structures*, AS4100-1998, Standards Association of Australia, Australian Institute of Steel Construction, Sydney, Australia.

Schaffer, B.W. (2003). “Cold-Formed Steel Design by the Direct Strength Method: Bye-Bye Effective Width,” *Proceedings*, Structural Stability Research Council, Annual Technical Session and Meeting, Univ. Missouri, Rolla, MO., 357-377.

SSRC (1998). *Guide to Stability Design Criteria for Metal Structures*, T.V. Galambos (ed.), Structural Stability Research Council, Wiley Interscience, New York, NY, 911 pp.

Trahair, N.S. (1977). “Lateral Buckling of Beams and Beam-Columns,” Chapter 3 in *Theory of Beam-Columns,* Vol. 2, W.F.Chen and T. Atsuta (ed.), McGraw-Hill, NY.

White, D.W. and Barth, K.E. (1998). “Strength and Ductility of Compact-Flange I Girders in Negative Bending,” *Journal of Constructional Steel Research*, 45(3), 241-280.

White, D.W. and Chang, C.-J. (2005). “General Design-Oriented Procedure for Calculation of Lateral-Torsional Buckling Effective Length Factors,” Structural Engineering, Mechanics and Materials Report No. 30, School of Civil and Environmental Engineering, Georgia Insitutute of Technology, Atlanta, GA.

White, D.W. and Jung, S.-K. (2003a). “Simplified Lateral Torsional Buckling Equations for I- and Channel-Section Members” Structural Engineering, Mechanics and Materials Report No. 24a, School of Civil and Environmental Engineering, Georgia Insitutute of Technology, Atlanta, GA.

White, D.W. and Jung, S.-K (2003b). “The Effect of Web Distortion on the Lateral-Torsional Buckling Strength of I-Beams,” Structural Engineering, Mechanics and Materials Report No. 24c, School of Civil and Environmental Engineering, Georgia Insitutute of Technology, Atlanta, GA.

White, D.W. and Jung, S.-K. (2004). “Unified Flexural Resistance Equations for Stability Design of Steel I-Section Members – Uniform Bending Tests,” Structural Engineering, Mechanics and Materials Report No. 28, School of Civil and Environmental Engineering, Georgia Institute of Technology, Atlanta, GA.

White, D.W. and Kim, Y.D. (2004). “Unified Flexural Resistance Equations for Stability Design of Steel I-Section Members – Moment Gradient Tests,” Structural Engineering, Mechanics and Materials Report No. 29, School of Civil and Environmental Engineering, Georgia Institute of Technology, Atlanta, GA.

White, D.W., Barker, M. and Azizinamini, A. (2004). "Shear Strength and Moment-Shear Interaction in Transversely-Stiffened Steel I-Girders," Structural Engineering, Mechanics and Materials Report No. 27, School of Civil and Environmental Engineering, Georgia Institute of Technology, Atlanta, GA.

APPENDIX A – NOTATION

A	Total cross-sectional area, in^2 (mm^2)
A_{fc}	Area of compression flange, in^2 (mm^2)
A_{fillet}	Area of each of the two web-to-compression flange fillets, generally taken equal to zero for welded I-shapes, in^2 (mm^2)
A_{rs}	Area of slab reinforcing steel, in^2 (mm^2)
A_{wc}	Area of web in flexural compression, D_ct_w, in^2 (mm^2)
B_1	Variable used in calculating the buckling moment for a singly-symmetric I-section member per Eq. (22), defined by Eq. (25)
B_2	Variable used in calculating the buckling moment for a singly-symmetric I-section member per Eq. (22), defined by Eq. (27)
C_b	Moment-gradient factor for lateral-torsional buckling
C_w	Warping constant, in^6 (mm^6)
D	Depth of the web; clear distance between the flange plates, in (mm)
D_c	Depth of the web in compression; distance from the cross-section centroid to the inside face of the compression flange, in (mm)
E	Modulus of elasticity of steel, 29 000 ksi (200 000 MPa)
F_{cr}	Elastic critical stress, ksi (MPa)
$F_{cr(exact,\ beam\ theory)}$	Elastic critical stress determined from the rigorous open-wallled section beam theory equations, including the exact determination of the coefficient of monosymmetry β_x
F_{max}	Maximum potential flexural resistance in terms of the compression flange stress, ksi (MPa)
F_y	Specified minimum yield stress, ksi (MPa)
F_{yr}	Compression flange flexural stress corresponding to the nominal onset of yielding at the extreme fibers in compression or tension, including compression flange residual stress effects
F_{yrs}	Yield strength of slab reinforcing steel, ksi (MPa)
G	Shear modulus of elasticity of steel, 11 200 ksi (77 220MPa)
I_x	Moment of inertia about the major axis of bending, in^4 (mm^4)
I_y	Moment of inertia about the minor-axis of bending, in^4 (mm^4)
I_{yt}	Moment of inertia of the tension flange about the plane of the web, in^4 (mm^4)
I_{yc}	Moment of inertia of the compression flange about the plane of the web, in^4 (mm^4)
J	St. Venant torsion constant, in^4 (mm^4)
K	Effective length factor for lateral-torsional buckling
K_y	Effective length factor for lateral-torsional buckling associated with minor-axis flexural restraint
K_z	Effective length factor for lateral-torsional buckling associated with warping restraint
L_b	Laterally unbraced length; length between points braced against lateral displacement of the compression flange, or between points braced to prevent twist of the cross-section, in (mm)
L_p	Limiting laterally unbraced length to achieve the maximum potential flexural resistance of the section, uniform moment case (C_b = 1.0), in (mm)
L_r	Limiting laterally unbraced length to achieve the onset of yielding in uniform bending (C_b = 1.0) at the extreme fibers in compression or tension, with consideration of compression flange residual stress effects
M_{cr}	Elastic buckling moment, kip-in (N-mm)
M_{max}	Maximum potential flexural resistance, kip-in (N-mm)
M_n	Nominal flexural strength, kip-in (N-mm)
M_p	Plastic bending moment about the axis under consideration, kip-in (N-mm)

M_{yc} Yield moment corresponding to the onset of yielding at the extreme compression fiber from an elastic stress distribution, kip-in (N-mm)

M_{yr} Yield moment capacity considering compression flange residual stress effects, $F_{yr}S_{xc}$, kip-in (N-mm)(?)

S_{xc} Elastic section modulus corresponding to the extreme compression fiber, in^3 (mm^3)

b_f Flange width, doubly-symmetric I-shapes and channels; width of the applicable flange, singly-symmetric I-shapes, in (mm)

b_{fc} Width of a rectangular compression flange, in (mm)

d Total depth between the extreme fibers of the flange elements perpendicular to the major axis of bending, in (mm)

h Distance between the centroids of the flange elements perpendicular to the major axis of bending, in (mm)

h_c Distance from the centroid of the cross-section to the mid-thickness of a rectangular compression flange, in (mm)

r_E Equivalent column radius of gyration corresponding to elastic lateral-torsional buckling strength, in (mm)

$r_{E(JL_b^2=0)}$ Equivalent column radius of gyration evaluated in the limit that JL_b^2 approaches zero, in (mm)

$r_{E(JL_b^2=0,\,sym)}$ Equivalent column radius of gyration evaluated in the limit that JL_b^2 approaches zero, specialized to a doubly-symmetric I-section, in (mm)

r_t Radius of gyration for lateral-torsional buckling defined by Eq. (3), in (mm)

r_{yc} Radius of gyration of the compression flange taken about the y axis, in (mm)

t_f Flange thickness, doubly-symmetric I-shapes and channels; thickness of the applicable flange, singly-symmetric I-shapes, in (mm)

t_{fc} Thickness of a rectangular compression flange, in (mm)

t_w Thickness of the web, in (mm)

y_o distance from the cross-section neutral axis to the shear center, negative if the larger flange is in compression, in (mm)

α Coefficient used in calculating the shear center location y_o and the warping constant C_w for a singly-symmetric I-section, defined by Eq. (12)

β_x Coefficient of monosymmetry, defined by Eqs. (18)

ν Poisson's ratio of steel, 0.3